atmosphere

MDPI

Article

Measuring Ammonia Concentration Distributions with Passive Samplers to Evaluate the Impact of Vehicle Exhaust on a Roadside Environment in Tokyo, Japan

Hiroyuki Hagino

Japan Automobile Research Institute (JARI), 2530 Karima, Tsukuba 305-0822, Ibaraki, Japan; hhagino@jari.or.jp

Abstract: Evaluating the impact on roadside environments of NH_3 from vehicle emissions is important for protecting the ecosystem from air pollution by fine particulate matter and nitrogen deposition. This study used passive samplers to measure NH_3 and NO_X at multiple points near a major road to observe the distribution of these gases in the area. The impact of NH_3 emitted from vehicles on a major road on the environmental concentration of NH_3 at different distances from the roadside was found to be similar to that of NO_X and NO_2. The concentration of NH_3 rapidly decreased due to dilution and diffusion within approximately 50 m of the road, and after 100 m the concentration remained almost the same or decreased slowly. Furthermore, CO_2 observations taken in the same period along the roadside and in the background yielded a vehicular emission factor of 4–50 mg/km for NH_3, which is comparable with previous research. This emission factor level contributes 4–11 ppb to the NH_3 concentrations in roadside air through the dilution and diffusion process. A correlation was found between the emission factors of NH_3 and NO_X that was different from the trade-off relationship seen when single-vehicle exhaust is measured.

Keywords: diffusive sampler; distance attenuation; emission rate; automotives

Academic Editors: Eui-Chan Jeon and Seongmin Kang

Received: 29 March 2025
Revised: 25 April 2025
Accepted: 28 April 2025
Published: 29 April 2025

Citation: Hagino, H. Measuring Ammonia Concentration Distributions with Passive Samplers to Evaluate the Impact of Vehicle Exhaust on a Roadside Environment in Tokyo, Japan. *Atmosphere* **2025**, *16*, 519. https://doi.org/10.3390/atmos16050519

1. Introduction

Ammonia (NH_3) gas is reduced nitrogen, and it is emitted into the atmosphere from various sources, with agriculture accounting for more than 81% of the global total emissions [1]. Satellite observation data has revealed not only the variety of emissions sources but also the spatial distribution of NH_3 emissions [2]. Indeed, it has been shown that the NH_3 concentration in cities around the world increased by 1.2%/yr between 2008 and 2019 [3]. The potential direct impact of NH_3 on the health of the general public in urban areas is not fully explained in the scientific literature, but systematic literature reviews have shown that NH_3 exposure may directly result in decreased lung function, irritation of the throat and eyes, increased coughing and sputum discharge, and early onset of asthma in infants [4].

NH_3 in the atmosphere reacts with acidic gases to form ammonium salts, which can increase the concentration of fine particles in the atmosphere [1–8]. In addition, particulate ammonium formed from NH_3 can be transported far from the source [7,9], and semi-volatile ammonium salts (e.g., Equation (1)) can return to NH_3 under specific meteorological and chemical conditions, such as concentration, temperature, and humidity [10–13].

$$NH_3 + HNO_3 \leftrightarrows NH_4NO_3 \quad (1)$$

NH_3 is highly reactive and is quickly removed, so its concentration decreases rapidly as it moves away from the source [14]. However, even at low concentration levels, NH_3 gas has been found to have a direct negative impact on plant communities, and a critical level of 1 $\mu g/m^3$ (1.4 ppb at 20 °C and 1 atm standard conditions) has been proposed to protect vegetation [15].

It has long been known that NH_3 in the atmosphere is emitted from biological processes in soil, biomass combustion, ammonia-based chemical fertilizers, sewage treatment plants, and the decomposition process of animal waste [7,16]. Since the introduction of three-way catalysts (TWCs) in the 1980s, attention has focused on the contribution of NH_3 emissions from gasoline-powered vehicles to atmospheric NH_3 concentrations [17–22]. TWCs are honeycomb-shaped ceramics coated with rare earth metals such as palladium (Pd), platinum (Pt), and rhodium (Rh). They are designed to control the emission of carbon monoxide (CO), unburned hydrocarbons (HC), and nitrogen oxides (NOx) from gasoline vehicles through a series of chemical oxidation–reduction reactions that occur on the surface of the catalyst. Thus, a TWC oxidizes CO and unburned HC compounds into carbon dioxide (CO_2) and water (H_2O) and reduces NO_X such as nitric oxide (NO) to nitrogen gas (N_2) [23–27]. When NO compounds are excessively reduced beyond the capacity to form N_2 gas on the surface of the TWC, NH_3 is formed, which is mainly related to the reaction between NO and H_2 [17–21,28]. This process usually begins with the water–gas shift reaction between CO and H_2O, which produces CO_2 and H_2 (Equation (2)), and NH_3 is formed as a result of the reaction between the produced H_2 and NO (Equations (3) and (4)).

$$CO + H_2O \rightarrow CO_2 + H_2 \quad (2)$$

$$2\,NO + 2\,CO + 3\,H_2 \rightarrow 2\,NH_3 + 2\,CO_2 \quad (3)$$

$$2\,NO + 5\,H_2 \rightarrow 2\,NH_3 + 2\,H_2O \quad (4)$$

Factors that may affect NH_3 formation in TWCs include aggressive driving [29–31], failure to maintain a stoichiometric air–fuel ratio [18,19,30–32], ambient temperature and engine temperature [33], and the age and model year of the TWC [34–38]. The efficiency of the TWC depends on the air–fuel ratio, and there is a narrow operating range around the stoichiometric ratio of air and fuel ($\lambda = 1$) where the TWC operates most efficiently. For this reason, fuel combustion in gasoline vehicles is generally controlled by a lambda sensor to achieve $\lambda = 1$, but aggressive driving can change λ. During lean combustion at $\lambda > 1$, NOx emissions usually increase, while during fuel-rich conditions of $\lambda < 1$, NH_3 emissions increase, so in general, there is a trade-off relationship between NOx and NH_3 emissions [38]. Another known cause of NH_3 emission is NH_3 slip (emission of unreacted NH_3 into the atmosphere due to excessive supply) on urea selective catalytic reduction (SCR) catalysts, which are used to reduce NOx emissions from diesel vehicles [39,40]. Therefore, to understand the complex dynamics of NH_3 concentrations in urban air and provide evidence of the effectiveness of NH_3 mitigation strategies that have been reported in previous studies e.g., [8], it is necessary to consider the impact of vehicle traffic on amounts of NH_3 in the surrounding environment.

Although many papers have been published on monitoring NH_3 in the atmosphere, there are still many issues to be addressed. Because the concentration of NH_3 varies greatly on spatial and temporal scales due to the rapid deposition of this molecule and its reactivity in the atmosphere, high time-resolution measurements using continuous analyzers have been attempted but suffer from measurement uncertainty depending on which analysis technology is used [41]. In addition, there are no standardized quality control/quality assurance procedures for measuring NH_3 and currently no established traceability or international guidelines to support measurements [42]. Passive samplers, which are a

classic method for measuring NH_3 [43–49], rely on the diffusion of the target gas onto a surface where it is chemically trapped by an adsorbent. Measurement uncertainty arises both from the preparation of the sampler and in the laboratory analysis, as well as the environmental exposure factors [43–49]. Most studies follow European standard diffusion sampler methodology EN 17346:2020 *Ambient air—Standard methods for the determination of NH_3 concentration using diffusion samplers* [50]. Examples of commercially available passive samplers include the Stream Sampler (Kogawa Seisakusho, Hyogo, Japan) and the Adaptive Low-cost Passive High Absorber (ALPHA) Sampler (Centre for Ecology and Hydrology, Edinburgh, UK). Because passive samplers take samples at a fairly low frequency (from one week to one month), the results obtained are low time-resolution measurements—average values observed over a long period of time—as opposed to those obtained by numerous types of continuous analyzer that respond to rapid concentration changes due to deposition and reactions in the atmosphere. Passive samplers are inexpensive and do not require a power supply, making them suitable for use in both urban and remote areas, where they can be used to measure at fine spatial resolutions and understand spatial variability. Consequently, previous studies using passive samplers have provided a wide range of knowledge about spatial distributions of air pollutant concentrations [51–53]. However, the components that can be measured using passive sampling are limited to those with high reactivity (such as NH_3, NO_2, and O_3), making it difficult to measure CO_2, an inert gas that needs to be measured in parallel to evaluate NH_3 emissions from vehicles in real atmospheric environments. Research that uses expensive continuous analyzers to provide CO_2 measurements is limited.

To investigate the effects of vehicle exhaust gases, this study used passive samplers that do not require a battery to determine the spatial distribution of NH_3 concentrations in a roadside environment. Furthermore, we determined the emission levels from vehicle exhaust gases by simultaneously measuring roadside and background CO_2 using a portable, battery-powered, low-cost sensor. The findings of this research are discussed in detail, comparing them with past research. The NH_3 emission factor of several tens of milligrams per kilometer observed by this study was found to contribute to the NH_3 concentration in roadside environments at a level of several parts per billion.

2. Materials and Methods

2.1. Locations

This study was conducted along a major road in the Tokyo metropolitan area, Japan. Tokyo, the capital of Japan, is one of the major urban areas in the world [54]. According to the latest statistics on vehicle fuel consumption in 2023 [55], Tokyo is the prefecture in Japan with the highest consumption of vehicle fuel, accounting for 5.4% (2,298,961/42,970,264 kL/yr) of gasoline, 4.7% (1,159,338/24,853,290 kL/yr) of diesel, and 1.7% (74,734/4,376,770 kL/yr) of liquefied petroleum gas consumed nationwide. Although there are no specific environmental policies related to NH_3 emissions in effect in Tokyo, it has been shown that the decrease in NH_3 concentrations during the 2020 Tokyo COVID-19 lockdown was mainly due to reductions in emissions from vehicles (20%) and humans (80%) [56]. Ring Road No. 8 (National road No. 311) is one of the major traffic arteries in the Tokyo metropolitan area, and cumulus clouds are frequently observed directly above it as it runs north–south on the west side of a densely populated urban area [54], making it an appropriate observation point for investigating both the urban climate and air pollution in a busy urban area.

To measure the planar concentration distribution of NH_3 and NO_X, passive samplers were installed at 20 sites (Figure 1 and Table 1) in the area surrounding a major road in Tokyo. According to Japanese traffic census data [57–59], the traffic volume on Ring Road

No. 8 near Nogemachi Park is approximately 52,000 vehicles per day, with a large-vehicle ratio of 17.2% (more details can be found in previous studies [60–62]).

Figure 1. Sampling locations. (**a**) Passive sampler setup at Site 1, and a close-up view of the sampling device (inset). (**b**) Locations of passive samplers at Sites 0 to 19.

Passive samplers were placed at varying distances (0–50 m from the road boundary line) around a central observation point (N 35°36′22.60″, E 139°38′33.71″) referred to as the Noge air quality monitoring station [61], which is located beside Ring Road No. 8. The locations were selected from among at least 10 points (i.e., at least 50% of the measurement points), and were selected to ensure that the samplers could be installed at 2.5 m above the ground to be out of reach of pedestrians. Samplers were attached to streetlights along the main road, on lampposts in the park area, and on telegraph poles in the residential area, and observations were carried out. This study determined the emission factors (emission levels) from vehicle exhaust gases in a twin-site study by simultaneously measuring roadside and background CO_2 and NH_3. To additionally measure the background urban atmosphere

not directly affected by roadside air, measurements of air pollutants taken at a general monitoring station located approximately 6 km from the roadside of this study were accessed online (measurement station code: 13112010, Setagaya air quality monitoring station, N 35°38′48.12″, E 139°39′11.42″) [63,64].

Table 1. Locations of passive samplers used in this study.

Site	Location	Distance from Road	Latitude	Longitude
0	Noge Station	3.23 m	N 35°36′22.60″	E 139°38′33.71″
1	Streetlight	0.55 m	N 35°36′23.10″	E 139°38′32.88″
2	Streetlight	0.55 m	N 35°36′22.40″	E 139°38′34.80″
3	Streetlight	0.55 m	N 35°36′21.85″	E 139°38′36.87″
4	Streetlight	0.65 m	N 35°36′22.69″	E 139°38′35.95″
5	Streetlight	0.65 m	N 35°36′23.26″	E 139°38′34.06″
6	Pedestrian Bridge	1.20 m	N 35°36′23.93″	E 139°38′32.68″
7	Pedestrian Bridge	1.90 m	N 35°36′24.58″	E 139°38′30.81″
8	Lamppost	16.58 m	N 35°36′22.69″	E 139°38′31.80″
9	Lamppost	60 m	N 35°36′21.35″	E 139°38′31.25″
10	Lamppost	122 m	N 35°36′19.63″	E 139°38′29.77″
11	Lamppost	9.50 m	N 35°36′21.86″	E 139°38′35.35″
12	Lamppost	78 m	N 35°36′19.72″	E 139°38′34.73″
13	Lamppost	98 m	N 35°36′19.09″	E 139°38′34.72″
14	Telegraph Pole	9.15 m	N 35°36′23.70″	E 139°38′33.48″
15	Telegraph Pole	67 m	N 35°36′25.41″	E 139°38′34.28″
16	Telegraph Pole	98 m	N 35°36′26.55″	E 139°38′34.70″
17	Telegraph Pole	17.2 m	N 35°36′22.78″	E 139°38′38.15″
18	Telegraph Pole	57 m	N 35°36′23.99″	E 139°38′38.55″
19	Telegraph Pole	104 m	N 35°36′25.60″	E 139°38′38.76″
20	Setagaya Station	Building Rooftop	N 35°38′48.12″	E 139°39′11.42″

2.2. Sampling

NH_3 and NO_X were measured using passive samplers (Figure 2) with reference to previous studies that showed the method was consistent with conventional continuous measurement and the Denuder method [43–49,53]. However, there are methodological limitations and uncertainties inherent in passive sampling, which can be attributed to fluctuations in the blank (i.e., unused collection material); to minimize the potential for these fluctuations, the collection period in this study was set at two weeks.

NH_3 concentration was measured using a short-term passive sampler (Figure 2a) (OG-KN-S, Ogawa & Co., Ltd., Hyogo, Japan) [65] inserted into a rain shelter (OG-SN-S, Ogawa & Co., Ltd., Hyogo, Japan) 2.5 m above the ground. The sampling period was one week. The filter paper (OG-SN-17, Ogawa & Co., Ltd., Hyogo, Japan) was removed from the sampler after collection, extracted with pure water, and the ammonium ion (NH_4^+) concentration was measured using ion chromatography (Integrion RFIC system, Thermo Fisher Scientific Inc., Waltham, MA, USA). The NH_3 concentration was calculated from this value using a calibration curve prepared separately and then corrected using temperature and humidity data [43–49,53] from the Japan Meteorological Agency's Tokyo Regional Meteorological Office [66] for the study periods. The method used to calculate NH_3 atmospheric concentration using passive sampling is described in Appendix A [65].

NO_X was measured using a long-term passive sampler (OG-KN-S, Ogawa & Co., Ltd., Hyogo, Japan) for measuring NO_2 and NO_X (Figure 2b) and filter papers impregnated with reagents, triethanolamine (OG-SN-10) for NO_2 and 2-phenyl-4,4,5,5-tetramethylimidazoline-3-oxide-1-oxyl (OG-SN-11) for NO_X. The sampling period was one week. The extract with pure water was then colored using Salzmann's reagent, and the

absorbance at a wavelength of 545 nm was measured. The NO_2 and NO_X concentrations were calculated from these absorbance values using a calibration curve prepared separately and then corrected in the same way as the NH_3 concentrations [43–49,53]. The method used to calculate NO_2 and NO_X atmospheric concentrations using passive sampling is described in Appendix B [65].

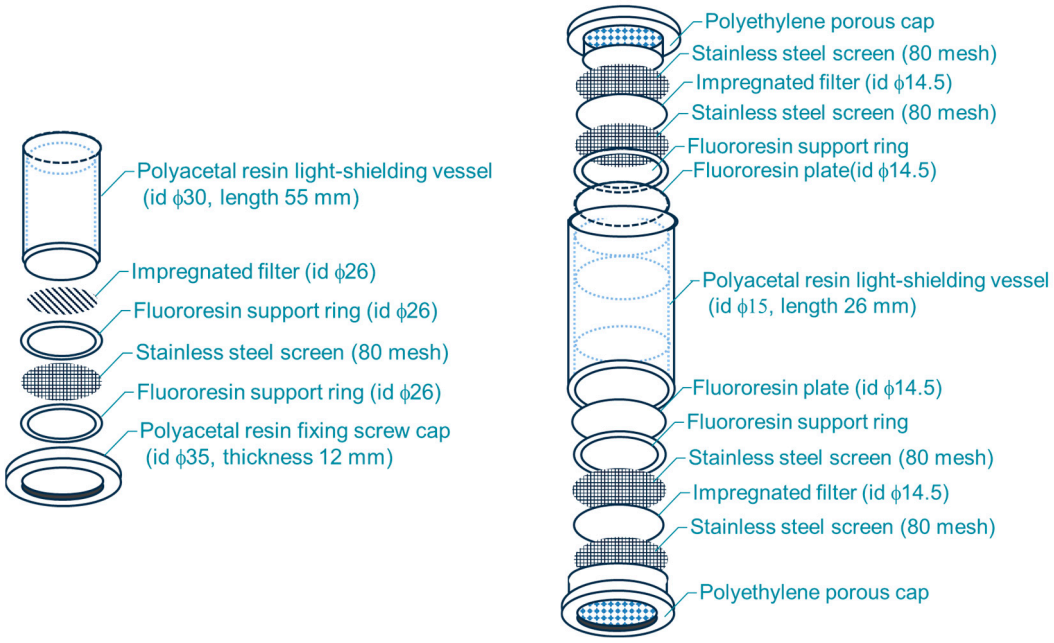

Figure 2. Schematic diagrams of passive samplers for (**a**) NH_3 and (**b**) NO and NO_X.

Sampling using the passive samplers was carried out twice on consecutive weeks in each of the four seasons: Autumn-1 (18 to 25 October, 2017), Autumn-2 (25 October to 1 November 2017), Winter-1 (17 to 24 January 2018), Winter-2 (24 to 31 January 2018), Spring-1 (9 to 16 May 2018), Spring-2 (16 to 23 May 2018), Summer-1 (18 to 25 July 2018), and Summer-2 (25 July to 1 August 2018) to correspond with the monitoring period for $PM_{2.5}$ component analysis designated by the Japanese Ministry of the Environment [67].

Low-cost CO_2 sensors (TR-76Ui, T&D Corporation, Matsumoto, Nagano, Japan) were used to roughly measure the effects of vehicle emissions at only two locations: near the roadside where a power supply could be used (Noge Station) and in the background at the general monitoring station in Setagaya. The CO_2 was measured continuously for two weeks with a one-minute resolution during the collection periods by passive sampler.

Microsoft M365 Excel was used to conduct the statistical analysis and construct scatter plots. Pearson product-moment correlation coefficients, calculated by the same software, were used to examine correlations.

3. Results and Discussion

3.1. Spatial Patterns in Concentrations of NH_3 and NO_X

The relationship between distance from the road boundary and concentration is shown in Figure 3, combining all measurements taken at Sites 0–19 in Table 1. The results for all seasons investigated in this study show that the concentrations of NH_3 and NO_X decreased rapidly up to about 50 m from the road, and beyond 100 m they either remained more or less the same or decreased gradually. The ratio of the highest concentration along the road to the background concentration (Site 20, Setagaya station) shows that the concentrations

decreased by 90% ± 2% for NH_3, by 61% ± 9% for NO_2, and by 80% ± 6% for NO_X throughout all seasons.

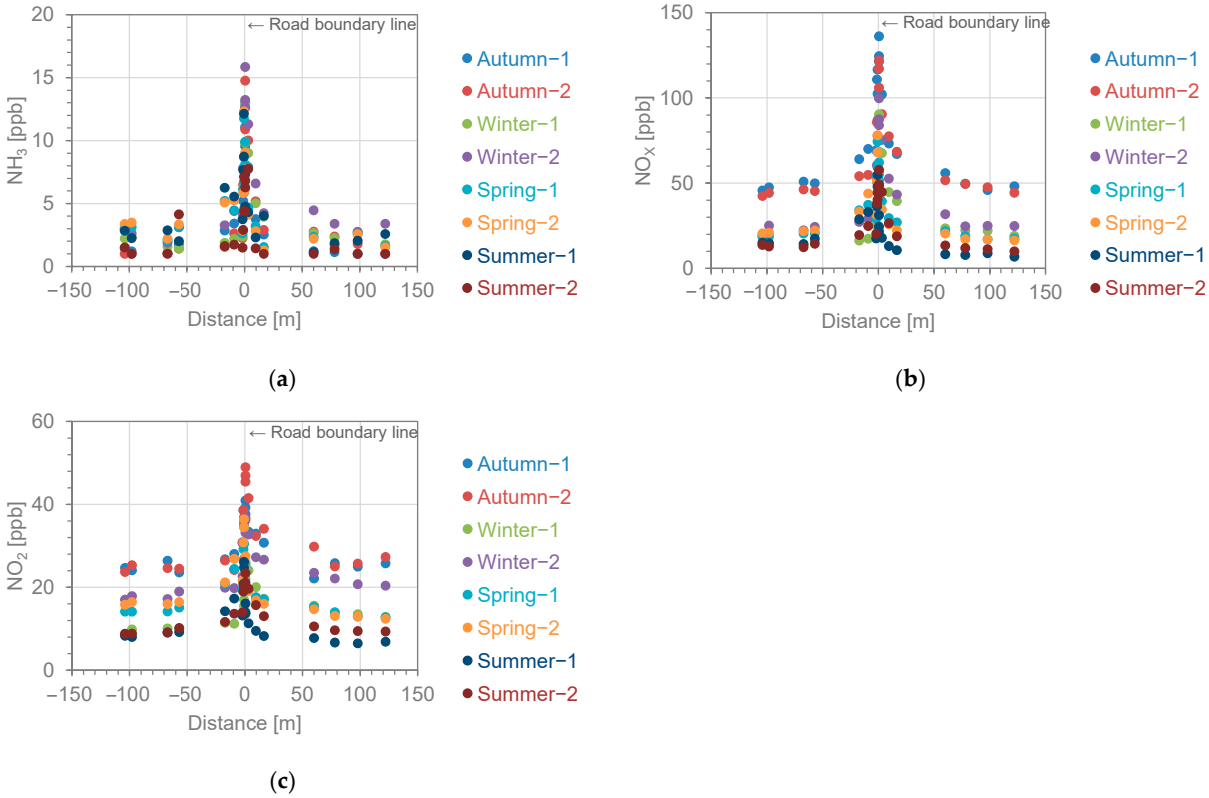

Figure 3. Concentrations measured at different distances (Sites 0–19) from Tokyo Ring Road No. 8. for (**a**) NH_3, (**b**) NO_X, and (**c**) NO_2. The distance from the road is shown with the upwind side as negative and the downwind side as positive. Zero meters in the figure indicates the road boundary line.

Several previous studies have shown that the concentrations of NH_3 and NO_2 decrease rapidly as you move away from the roadside. In one study that measured NH_3 in suburban roadside environments with different traffic volumes, a 99% decrease in concentration was observed at a distance of 20 m from the roadside [68]. Another study in suburban roadside environments found a 90% decrease in NH_3 concentration from background levels at a distance of 10 m from the roadside and a 90% decrease in NO_2 concentration at a distance of 15 m from the roadside [69]. When NH_3 and NO_X were measured in three roadside environments in urban areas, a reduction in concentration of approximately 80% from background levels several hundred meters away from the road was observed at a distance of 50 m from the roadside [70]. Despite the variation in the results found in these studies [68–70], NH_3 concentrations behaved in a similar way to NO_X and NO_2 concentrations across all the areas under observation, decreasing rapidly at around 50 m from a road, and then either remaining more or less the same or decreasing gradually after 100 m. The reason for the variation in the results of these studies is thought to be the differences in conditions, such as the types and numbers of vehicles driving on the roads under observation, the season, and the presence of obstructions [70]. For example, it was found that the NH_3 concentration was 140% higher on average at a distance of 12 km downwind from a major urban area than in the hinterland (upwind of the roadside) of roadside observations in the suburbs [71]. In addition, in urban areas, NH_3 concentrations at roadside locations were observed to be approximately 80% lower than at background locations [72]. Therefore, the observed reduction rate is likely to be affected by the difference between local and background concentrations of pollutants.

This study also found a high correlation between the increase in NH_3 concentration and those of NO_X (Figure 4a–d) and NO_2 (Figure 4e–h) (NO_X: r = 0.953 ± 0.039, NO_2: r = 0.909 ± 0.046). Unexpectedly, the correlations between NO_X or NO_2 and NH_3 were found to be weaker in the summer, and further investigation is needed to elucidate the reason for this finding. Relative to the regression lines for NH_3 concentration over the entire survey period, the slope of the regression line for NO_X concentration was 0.153 ± 0.024, with a relative standard deviation of 16%, and the slope of the regression line for NO_2 concentration was 0.479 ± 0.024, with a relative standard deviation of 21%. As shown in Equation (1), the generation of NH_3 due to the dissociation of NH_4NO_3 at high temperatures, such as through the pre-deposition of ammonium ion (NH_4^+) species together with water (dew, mist, etc.) on grassland or building walls under high relative humidity at night, is an important process that promotes evaporation in the morning [73,74]. However, in the summer, when temperatures are high, the atmosphere becomes more mixed in the vertical direction (i.e., the NH_3 concentration is diluted), such that dilution in the atmosphere is thought to be greater than the formation of NH_3 through the decomposition of NH_4NO_3 (Equation (1)), causing the NH_3 concentration to decrease. In a previous study [55], the concentration of NH_3 tended to be slightly higher in the winter than in the summer in an urban area of Tokyo. The scatter plots of NH_3, NO_X, and NO_2 (Figure 4) obtained in this study show a high correlation and a slope that is generally consistent regardless of the season, indicating that the exchange of gases and particles around the roadside and the effects of evaporation from deposited ion species are within the range of variation to be expected in observations taken using passive samplers with low time-resolution measurements.

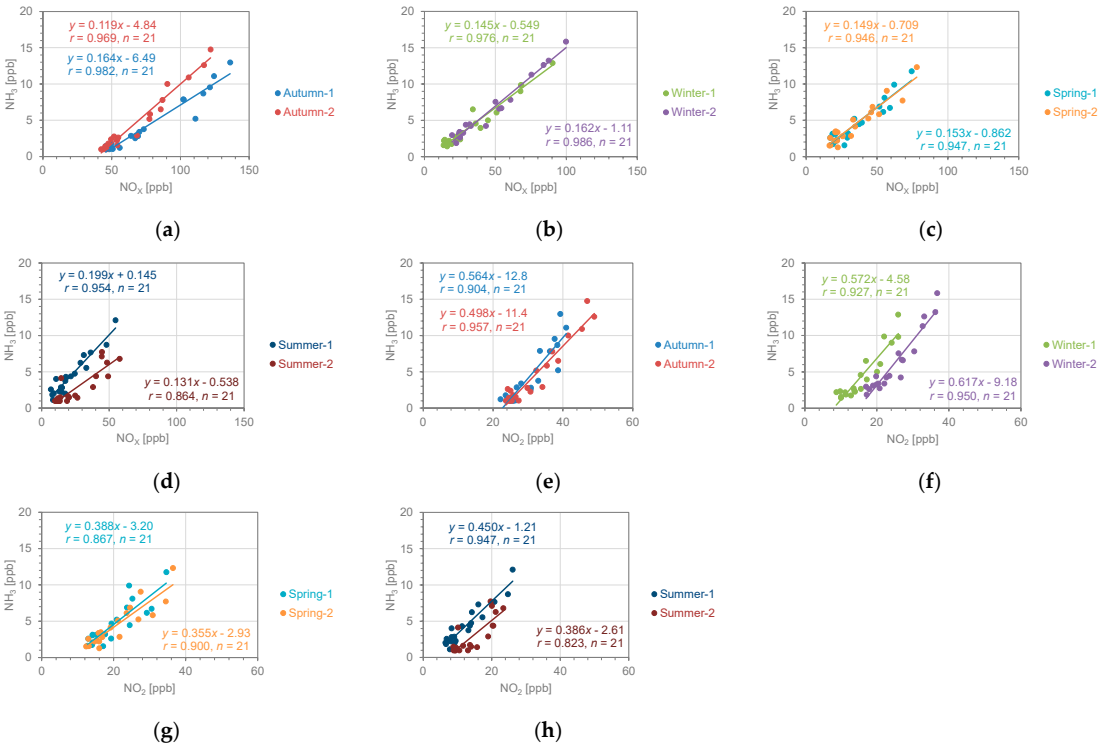

Figure 4. Scatter plots of NO_X and NO_2 against NH_3 measured at all locations, stratified by season. The relationship between NOx and NH3 is shown for (**a**) autumn, (**b**) winter, (**c**) spring, and (**d**) summer. The relationship between NO2 and NH3 is shown for (**e**) autumn, (**f**) winter, (**g**) spring, and (**h**) summer.

In line with the findings of previous studies [70], the current study found that the impact of NH_3 emitted from vehicles driving on major roads on environmental concentrations

at different distances from the roadside was in the same range as that of NO_X and NO_2, and that NH_3 concentrations decreased rapidly due to dilution and diffusion within about 50 m of the road and remained almost unchanged or decreased slowly after 100 m.

Nitrogen monoxide (NO) contained in NO_X (i.e., NOx − NO) is attracting attention as an indicator of primary emissions [75,76]. According to the results of simultaneous measurements taken every second at four of the locations used in the present study, 40% of atmospheric NO at the study location is rapidly oxidized to NO_2 by O_3 (Equation (5)) [76] during advection from the road boundary (0 m) to a point 20 m away [75].

$$NO + O_2 \rightarrow NO_2 + O_2 \quad (5)$$

In the present study, a two-week time resolution was used. However, primary NO emissions are rapidly oxidized. To address this, NO concentrations were included in NO_X concentrations. At the roadside (Site 0), overall NO_2/NO_X ratios of 33–63% were observed, which when stratified by season provided the following ratios: winter (33–46%), autumn (33–43%), summer (44–63%), and spring (49–55%). In the urban background (Site 20), the ratios were higher than along the roadside for each season: winter (61–62%), autumn (79–81%), summer (56–75%), and spring (78–82%). These results are consistent with previous studies [76] indicating that the NO_2/NO_X ratio is higher in spring and summer when reactions with O_3 are progressing [76].

3.2. Comparison with NH_3 Concentrations in Other Regions and Periods

Table 2 and Figure A1 in Appendix C show the NH_3 concentration ranges found using passive samplers in this and previous studies conducted in other years and various regions. In roadside observations of vehicle exhaust emissions, NH_3 concentrations in other studies were observed to be in the range of 1–31 ppb [68–70], so the NH_3 concentrations of 4–11 ppb observed at the roadside (Site 0 in Table 1) in 2017–2018 in this study were within the concentration range of previous studies. The variation in NH_3 concentrations at the roadside in other studies depended on the region and length of observation rather than the year of observation. In particular, the highest NH_3 concentrations (32–129 ppb) were reported for measurements taken in road tunnels, where there are no sources other than vehicles and NH_3 concentration is not diluted. It is known that NH_3 is emitted from gasoline, diesel, and liquefied petroleum gas vehicles, and some of the nitrogen oxides emitted from vehicles are reduced to NH_3 by the TWC installed in the vehicle and released into the atmosphere [17–22]. Vehicle exhaust is recognized as one of the main sources of NH_3 in urban areas [77,78], and reports have shown that NH_3 emissions are increasing not only in areas with high vehicle density but also in agricultural areas [79,80]. Regarding background levels, Table 2 and Figure A1 show that the NH_3 concentration along the roadside tended to be high as that in one of the industrial city areas (6–11 ppb). The background NH_3 concentration in urban areas is reported to be 1–85 ppb, and in suburban and rural areas 1–78 ppb. The NH_3 concentration of 1–5 ppb observed in the urban background in this study (Site 20 in Table 1) was therefore within the concentration range of previous studies. The comparison of data in Table 2 and Figure A1 also show that the variation in NH_3 concentration in urban areas (1–85 ppb) was wider than the variation in NH_3 concentration in roadside environments (1–31 ppb).

In the locations shown in Table 2 and Figure A1, livestock areas and sewage treatment plants were the sources of the highest concentrations of NH_3 (266–8455 ppb), and a wide range of concentrations were observed in these environments. NH_3 emissions have also been reported from landfill sites and incineration facilities that process general waste generated in residential areas [81], from electronic cigarettes [82], and from plant combustion in urban areas [83]. To understand the various characteristics of NH_3 emissions, detailed data

on concentrations and their sources in each case is important. A potential source of NH_3 that has attracted attention in recent years is a technique for co-firing NH_3 to reduce CO_2 emissions from internal combustion engines in vehicles and coal-fired power plants [52]. Additionally, NH_3 emissions due to NH_3 slip are an example of NH_3 combustion [84,85]. Therefore, although it should be emphasized that the increase in NH_3 concentrations found in the present study between the background (i.e., concentrations more than 100 m distance from the road in Figure 3 and at Site 20) and the roadside (concentrations at 0 m distance from the road in Figure 3) is due to vehicle exhausts, it should also be noted that high NH_3 concentrations of non–motor vehicle origin may also be important.

Table 2. NH_3 concentration ranges measured in studies using passive samplers at various locations and in different periods.

Location	Region	Period	NH_3 [ppb] *1	Reference
Roadside	Tokyo, Japan	2017–2018	4–11	This Study
Roadside	Saitama, Japan	2005–2007	6–31	[70]
Roadside	London, UK	2006–2019	4–7	[86]
Roadside	Barcelona, Spain	2010–2011	1–25	[81]
Roadside	Gyeonggi, Korea	2020–2021	12–20	[87]
Roadside	2 sites, Korea	2022	8–26	[53]
Road tunnel	Beijing, China	2014–2015	32–129	[88]
Urban	Tokyo, Japan	2017–2018	1–5	This Study
Urban	2 sites, North America	2003–2014	1–4	[89]
Urban	Xi'an, China	2006–2007	1–52	[90]
Urban	Beijing, China	2008–2010	1–85	[91]
Urban	Barcelona, Spain	2010–2011	6–55	[81]
Urban	13 sites, China	2015–2016	4–41	[52]
Urban	New York, USA	2016–2017	0.1–5	[92]
Urban	Beijing, China	2019	13–32	[79]
Urban	Gyeonggi, Korea	2020–2021	4–23	[87]
Urban	3 sites, Korea	2022	2–24	[53]
Urban background	Gyeonggi, Korea	2020–2021	2–5	[87]
Urban and rural	Asia, Africa, and South America	1999–2001	1–20	[51]
Suburban	Edinburgh, UK	2006–2019	1–3	[86]
Suburban	Xi'an, China	2006–2007	1–78	[90]
Suburban	Colorado, USA	2010–2015	3–15	[93]
Rural	11 sites, North America	2003–2015	0.2–6	[52]
Rural	Beijing, China	2007–2010	1–43	[91]
Rural	Colorado, USA	2010–2015	1–8	[93]
Rural, remote	40 sites, China	2015–2016	0.4–25	[52]
Rural	New York, USA	2016–2017	0.2–5	[92]
Rural	Jeongeup, Korea	2019–2020	11–38	[94]
Rural	5 sites, Korea	2022	0.8–6	[53]
Industrial	Gyeonggi, Korea	2020–2021	6–11	[87]
Industrial	10 sites, Korea	2022	4–87	[53]
Agricultural	North Carolina, USA	2003–2004	5–21	[95]
Agricultural	Colorado, USA	2010–2015	5–104	[93]
Agricultural	Navarre, Spain	2013–2015	7–79	[96]
Agricultural	Nanjing, China	2015–2016	7–57	[52]
Agricultural	8 sites, Korea	2022	6–35	[53]
Livestock	Beijing, China	2014–2015	670–2129	[88]
Livestock	Gyeonggi, Korea	2020–2021	32–96	[87]
Livestock	7 sites, Korea	2022	15–266	[53]
Waste plants	Beijing, China	2014–2015	186–8455	[88]

*1: Reported concentrations of mass per volume ($\mu g/m^3$) were converted to ppb under standard conditions of 20 °C and 1 atm.

3.3. NH_3 Emission Factors

The NH_3 emission factors obtained in this study were calculated based on passive sampling of NH_3 and NO_X, and of CO_2 using low-cost sensors (see "Section 2.2. Sampling"). A comparison with NH_3 emission factors based on different approaches that require expensive and diverse equipment that can focus on different targets helps to clarify the bulk emission factors from vehicles in a given area. Therefore, Table 3 compares the NH_3 emission factors based on distance and fuel measured in this study, as calculated from the NH_3 to CO_2 conversion ratio, with the results of previous studies obtained from dynamometers, in tunnels, by remote sensing, and in on-road experiments.

Table 3. NH_3 emission factors for vehicles in other regions and periods.

Location or Target	Measurement Device	Year	NH_3 Emissions [mg/km/Vehicle]	Reference
Roadside, Tokyo, Japan	Passive sampler	2017–2018	4–50	This Study
Urban, Tokyo, Japan	Semi-continuous analyzer	2017	3.7–32	[97]
Van Nuys Tunnel, California, USA	Filter pack	1993	61	[32]
Caldecott Tunnel, California, USA	Denuder	1999	46–52	[98]
Gurbrist Tunnel, Switzerland	Continuous analyzer	2002	26–35	[99]
Jânio Quadros Tunnel, São Paulo, Brazil	Impinger	2011	20–64	[100]
Tunnel, Guangzhou, China	Semi-continuous analyzer	2013	216–119	[101]
Handan Tunnel, Shanghai, China	Passive	2014	23–52	[22]
On-road, California, USA	Remote sensing	1996	86–102	[102]
Gasoline vehicle	Chassis dynamometer	2002	2–110	[103]
Gasoline vehicle	Chassis dynamometer	2004	1–31	[104]
Gasoline vehicle	Chassis dynamometer	2006	3–256	[105]
Gasoline vehicle	Chassis dynamometer	2008	3–28	[31]
Gasoline vehicle	Chassis dynamometer	2014	4–70	[106]
Gasoline vehicle	Chassis dynamometer	2017	2–132	[107]
Gasoline vehicle	Chassis dynamometer	2018	5–53	[36]
Gasoline vehicle	Chassis dynamometer	2022	1–53	[108]
Gasoline vehicle	On road	2020	1–53	[109]
Diesel vehicle	On road	2020	1–32	[109]
Compressed natural gas vehicle	On road	2020	38–90	[109]
Gasoline vehicle	Emission inventory	2018	29–104	[80]
Diesel vehicle	Emission inventory	2018	0.6–1.7	[80]
Gasoline vehicle, Japan	Emission inventory	2020	0.1–95	[110]

Emission factors are also expressed as mg/kg-fuel normalized per CO_2 emission and mg/km normalized per driving distance. Emission factors used to create emission inventories, which are usually used as data to analyze the effectiveness of the vehicle emissions type certification process and emission regulations, express emissions in distance-based factors, such as grams per kilometer or per mile [111].

Methods for estimating emission factors from atmospheric observations have been summarized in a systematic literature review [112]. In this study, emission factors were estimated by Equation (6), which is based on that used for twin-site studies (i.e., simultaneous measurement of the roadside and background) [112]:

$$\text{Emission Factor} = \frac{\left([NH_3]_{road} - [NH_3]_{background}\right)}{\left([CO_2]_{road} - [CO_2]_{background}\right)} \times W_{CO_2} \times FC \quad (6)$$

where $[NH_3]_{road}$ and $[NH_3]_{background}$ are the NH_3 concentrations at road (Site 0) and background (Site 20) (mg/m^3); $[CO_2]_{road}$ and $[CO_2]_{background}$ are the CO_2 concentrations at road (Site 0) and background (Site 20) ($kg\text{-}CO_2/m^3$); W_{CO2} is the content of carbon in fuel ($kg\text{-}CO_2/L$), taking into account the proportion of gasoline and diesel vehicles; and FC is the distance-based fuel consumption volume (L/km), taking into account the proportion of gasoline and diesel vehicles.

W_{CO2} is estimated by Equation (7):

$$W_{CO_2} = W_{CO_2}(\text{Gasoline}) \times \frac{100 - P_{diesel}}{100} + W_{CO_2}(\text{Diesel}) \times \frac{P_{diesel}}{100} \quad (7)$$

where W_{CO2} (Gasoline) is the content of carbon in gasoline fuel (2.32 kg-CO_2/L) and W_{CO2} (Diesel) is the content of carbon in diesel fuel (2.49 kg-CO_2/L) [113], and P_{diesel} is the proportion of diesel vehicles (heavy-duty vehicles) (17.2%) [57].

FC is estimated by Equation (8):

$$FC = FC(\text{Gasoline}) \times \frac{100 - P_{diesel}}{100} + FC(\text{Diesel}) \times \frac{P_{diesel}}{100} \quad (8)$$

where FC (Gasoline) is the statistical estimate value for a gasoline vehicle (0.085 L/km) [114] and FC (Diesel) is the statistical estimate value for a diesel vehicle (0.220 L/km) [114].

Distance-based NH_3 emission factors for individual vehicles obtained in the past—from dynamometer experiments, in vehicle tracking studies on roads, and in emission inventories—vary widely from 0.1 to 256 mg/km (Table 3). In general, vehicles driven at aggressive driving cycles usually lead to an increase in the NH_3 emission factor [29,105,106], and the aging of the TWC and of the vehicle [35–37] also contribute to the large variation. The measurements taken in previous studies, both in road tunnels and by remote sensing, also showed a wide variation, ranging from 3.7 to 119 mg/km. The results of this study fell within the range of the wide variation in the results of previous experiments and in measurements taken under actual atmospheric conditions. In particular, the results of this study were generally consistent with the results of measurements taken at different locations and using different methods in urban atmospheres.

Measurements of NH_3 taken in road tunnels, on roads, and in urban air cover all types of vehicles, both gasoline and diesel vehicles. However, I view the impact of diesel vehicles on NH_3 emissions to be limited in this study. This is because heavy vehicles account for approximately 17.2% of the vehicles passing along the roadside in this study. In Japan, the introduction of SCR systems using urea for heavy trucks and other vehicles began in the mid-2000s [115]. SCR systems produce more NH_3 [39,40], and there is a possibility that they increase the emission factor of NH_3 from diesel vehicles. At the time this research was conducted in 2017, the number of diesel vehicles (heavy vehicles) sold in Japan with SCR systems installed was 634,000 vehicles [115], which is about 4% of the total number of vehicles owned in Japan (14,652,000 vehicles) [116]. Vehicles without SCR systems generally have low NH_3 emissions [36] and have little effect on the results of emissions, so in this study, the impact of diesel vehicles on NH_3 emissions would be limited.

It is reported that NH_3 emissions from urban soil in green spaces are highly likely to have contributed spikes in atmospheric NH_3 that occur after the morning rush hour [117]. The timing of the morning peak after the morning rush hour, as measured by a device with a one-hour time resolution, is consistent with the results of a previous study [117]. NH_3 emissions from soil are also partially dependent on the ambient temperature. However, a study that estimated the NH_3 emission coefficient by observing the NH_3 concentration in the general atmosphere of Tokyo suggested that the impact of emissions from urban soil in green spaces is small, as although emissions from green space soil may be a source of NH_3 in urban areas, they are insufficient to cause an NH_3 peak equivalent to or greater than that of annual vehicle emissions [97]. Therefore, although the NH_3 emission factor estimated in this study includes emissions from urban soil in green spaces, it is within the range of variation in observations taken using passive samplers at low time-resolution measurements.

This study has found some interesting results, including a correlation between the emission factors for NH_3 and NO_X calculated from measurements taken in the atmosphere (Figure 5). In this study, the use of passive samplers with low time-resolution measurements gave a bulk measurement (averaged result) in which the numbers of gasoline and diesel vehicles were mixed in a specific ratio, whereas previous studies have observed clear differences (both trade-offs and correlations) between the NH_3 and NO_X emission factors measured from gasoline and diesel vehicles individually [100]. Therefore, some explanation is needed of the factors involved in differences between the measured values observed in the atmosphere in this study and the measured values for individual vehicles. First, diesel vehicles emit much less NH_3 than gasoline vehicles but emit more NO_X. In the case of gasoline vehicles, the NO_X emitted from the engine is minimized by the reduction reaction in the TWC. Therefore, there is a trade-off relationship between NO_X and NH_3 emissions, meaning that it is difficult to completely suppress both NO_X and NH_3 emissions from certain vehicle types [38,100]. Second, it has also been reported that as the driving distance of gasoline vehicles increases, both NH_3 and NO_X emissions increase [38,100]. Under certain conditions in TWCs, excessive reduction of NO_X occurs, so the target product of N_2 is not obtained, and NH_3 is produced as an unintended byproduct (Equations (3) and (4)). The efficiency of a TWC depends on the air–fuel ratio, and combustion is controlled to ensure that the TWC operates within a narrow operating range where it is most efficient (air–fuel stoichiometric ratio of $\lambda = 1$). When components such as the catalyst surface and lambda sensor deteriorate over time, the air–fuel ratio may become difficult to control. In addition, when the catalyst deteriorates over time, the catalytic activity and oxygen storage capacity decrease, so the reduction efficiency decreases because there is insufficient O_2 for the redox reaction [38]. In Japan, the average age of passenger cars in 2017 was 12.91 years [118], and further research into emissions from vehicles in use will help to clarify the impact of reductions in TWC efficiency. Therefore, we consider that a combination of these effects is present in the correlation between the emission coefficients of NH_3 and NO_X found in the atmospheric observations at low time-resolution measurements taken in this study.

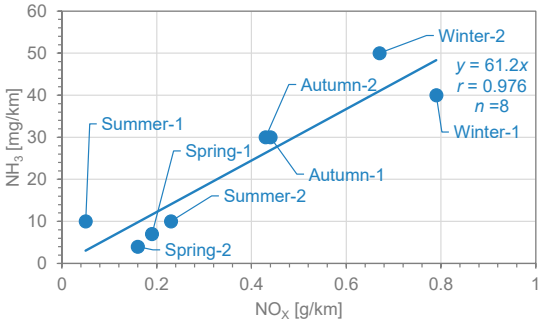

Figure 5. Comparison of NH_3 and NO_X emission factors.

In Figure 5, when comparing winter and summer, the emission factors for both NO_X and NH_3 were increased by more than four times in winter. This is roughly consistent with previous dynamometer measurements conducted at −7 °C and 23 °C that also showed an increase in NH_3 emission factor with decreasing temperature and was higher than the NH_3 emission ratio of 1.4–2.1 [107,108], which was attributed mainly to rich combustion during cold starts. The difference in the amplitude of the increase and decrease is thought to be due to differences in measurement accuracy, as the NH_3 concentration in this study was measured within a range of two orders of magnitude (4–11 ppb) at Roadside (Site 0).

The above comparison of results from previous studies and those found in this study emphasizes the need for further research on different parameters affecting NH_3 concentration to help estimate NH_3 emission factors for large volumes of vehicle activity. Further measurements in roadside environments along multiple roads with different average vehicle speeds, vehicle types, and traffic volumes will clarify the bias in the correlation between NH_3 and NO_X emission factors. In particular, Japan does not have any policies regarding ammonia measurement (such as the EU's Air Quality Directive [119]). This study highlights the importance of policy decisions based on the correlation between emission factor levels and the NH_3 concentration in roadside air, which was found here to contribute 4–11 ppb to the NH_3 concentration in roadside air through dilution and diffusion processes (i.e., the effect of halving the emission factor would be to halve the concentration of NH_3 in the air at multiple locations).

4. Conclusions

This study used passive samplers to observe NH_3 and NO_X and clarify the planar distribution around the road; that is, the attenuation of concentration with distance from the road. The research design highlights the potential for low-cost, multi-point observation as an evaluation tool that can contribute to improving the air quality of roadside environments. In addition, by adding CO_2 measurements using a low-cost sensor, it was shown that the values were within the range of reasonable vehicle emission factors, compared to the considerably large and varied measurement values of previous studies. A correlation found between the NH_3 and NO_X emission factors obtained in this study is contrary to the trade-off relationship between NH_3 and NO_X measured for individual vehicles in previous studies. The low time-resolution measurement method used in this study means that the average values represent the combined effects of gasoline and diesel vehicles, which both affect the emission factors in different ways. Even if regulations to mitigate the effects of NH_3 concentration are enforced on new and used vehicles, it will take a considerable amount of time for the effects of the regulations to be seen. For this reason, it will also be important to take temporary measures, such as updating road structures (for example, by installing soundproof walls and greening), urban structures (for example, by modifying urban structures to separate traffic networks for people and vehicles to reduce congestion), and traffic regulations. The research design used in this study demonstrates the potential for low-cost, multi-point observation as an evaluation tool that can contribute to improving the air quality of roadside environments.

Funding: This research received no external funding.

Institutional Review Board Statement: Not applicable.

Informed Consent Statement: Not applicable.

Data Availability Statement: The data published in this study are available on request with a letter of reasonable explanation to the corresponding author. No data have been made publicly available for data privacy reasons.

Acknowledgments: The author would like to thank the co-workers who supported the set-up and operation of the passive samplers. In addition, the authors would like to thank Akiyoshi Ito for his support in proofreading during the preparation of the draft manuscript. Passive sampler observations were conducted with the support of the Green Blue Corporation (Yokohama, Japan). Noge Station was implemented with the cooperation of Greenery Planning Division, Setagaya.

Conflicts of Interest: The author declares no conflicts of interest.

Appendix A. Calculation of NH_3 Atmospheric Concentration Using Passive Samplers

The NH_3 concentration (ppb) in the atmosphere was calculated from the amount of NH_3 collected on the filter paper (ng) and the exposure time by using the following equation [65]:

$$NH_3 = \omega NH_3 \times \alpha NH_3/t \quad \text{(A1)}$$

where ωNH_3 is the amount of NH_3 collected on the filter paper [ng], αNH_3 is the atmospheric NH_3 concentration conversion factor [ppb·min/ng], and t is the exposure time (collection time) [min].

The amount obtained by subtracting the blank amount (αNH_3), which was obtained by analyzing a filter paper that had not been exposed, was also used. This coefficient changes depending on the temperature, but it is hardly affected by temperature or atmospheric pressure. To ensure accurate measurements, the following equation was used to calculate the corrected coefficients [65]:

$$\alpha NH_3 = 87.6 \times (293/(273 + T))^{1.83} \quad \text{(A2)}$$

where T is the average temperature during collection [K].

Appendix B. Calculation of NO_X and NO_2 Atmospheric Concentrations Using Passive Samplers

The atmospheric concentrations of NO_X and NO_2 (ppb) were calculated using the following equations, based on the amounts (ng) of NO_X and NO_2 collected on the filter paper and the exposure time (min) [65]:

$$NO = \omega NO \times \alpha NO/t \quad \text{(A3)}$$

$$\omega NO = \omega NO_X - \omega NO_2 \quad \text{(A4)}$$

$$NO_2 = \omega NO_2 \times \alpha NO_2/t \quad \text{(A5)}$$

$$NO_x = NO + NO_2 \quad \text{(A6)}$$

where ωNO_X is the amount of NO_X collected on the NO_X collection filter paper [ng] and ωNO_2 is the amount of NO_2 collected on the NO_2 collection filter paper [ng].

ωNO_2 and ωNOx are values obtained by subtracting the blank amount, which was obtained by analyzing a filter paper that had not been exposed. The coefficients αNO [ppb·min/ng] and αNO_2 [ppb·min/ng] change with temperature, relative humidity, and atmospheric pressure. To ensure accurate measurements, the following equations were used to calculate the corrected coefficients [65]:

$$\alpha NO = 4.746 \times (4781.3 - T)/(474.2 - P \times RH)] \quad \text{(A7)}$$

$$\alpha NO_2 = 1.050 \times 106/(44.6 + T)/(206.4 + P \times RH)) \quad \text{(A8)}$$

$$P = (2P_N/(P_T + P_N))^{2/3} \quad \text{(A9)}$$

where RH is the average relative humidity during collection [%], T is the average temperature during collection [°C], P is the water vapor pressure correction coefficient, P_N is the water vapor pressure at 20 °C [17.535 mmHg], and P_T is the water vapor pressure at average humidity [mmHg].

Appendix C. NH_3 Concentration Ranges Measured in Studies Using Passive Samplers at Various Locations

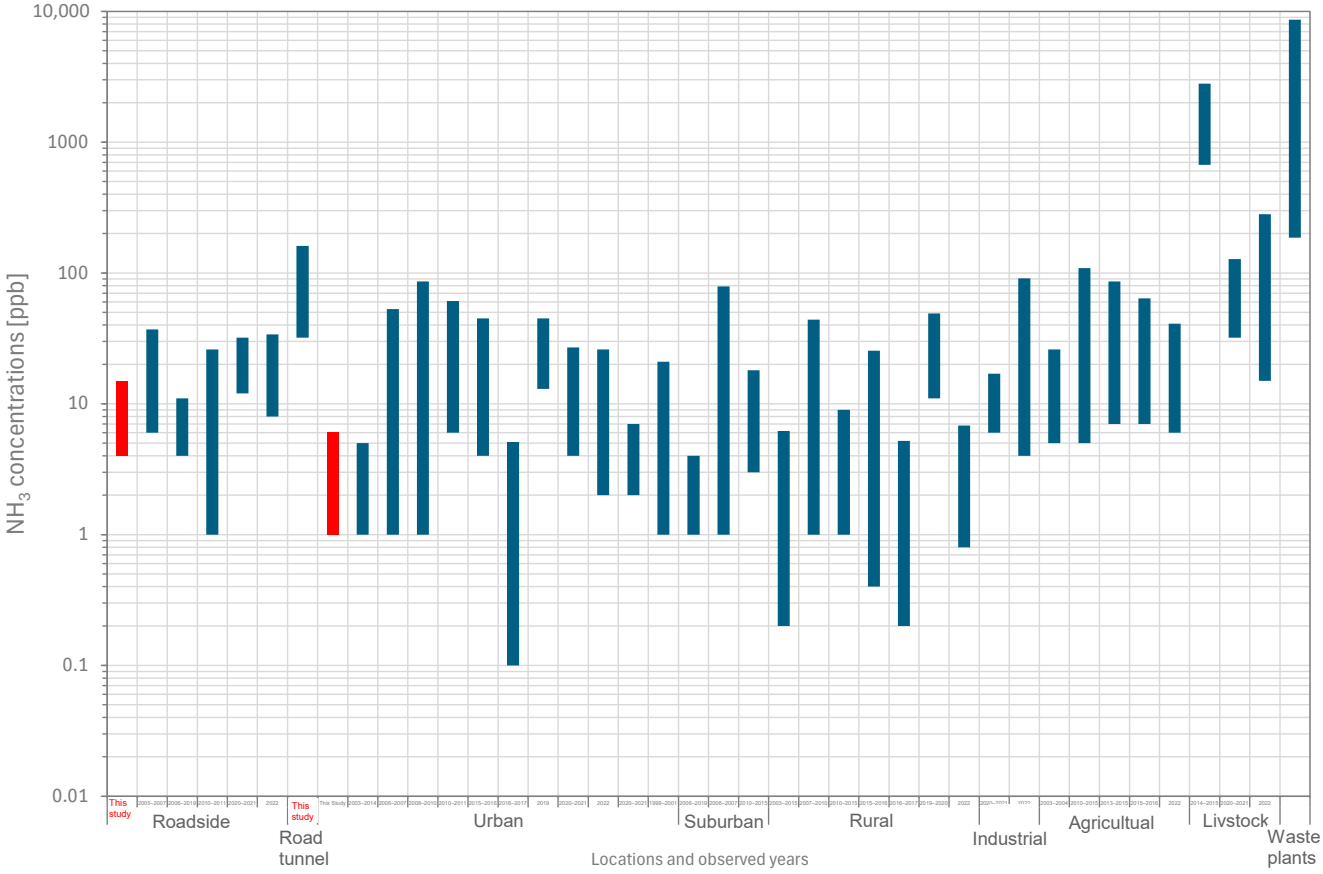

Figure A1. NH_3 concentration ranges measured in studies using passive samplers at various locations [47–49,64,67–76,81,87]. The red plot shows the data from this study.

References

1. Van Damme, M.; Clarisse, L.; Franco, B.; Sutton, M.A.; Erisman, J.W.; Kruit, R.W.; van Zanten, M.; Whitburn, S.; Hadji-Lazaro, J.; Hurtmans, D.; et al. Global, regional and national trends of atmospheric ammonia derived from a decadal (2008–2018) satellite record OPEN ACCESS RECEIVED Global, regional and national trends of atmospheric ammonia derived from a decadal (2008–2018) satellite record. *Environ. Res. Lett.* **2021**, *16*, 055017. [CrossRef]
2. Epps, A.; Dressel, I.M.; Guo, X.; Odanibe, M.; Fields, K.P.; Carlton, A.M.G.; Sun, K.; Pusede, S.E. Satellite Observations of Atmospheric Ammonia Inequalities Associated with Industrialized Swine Facilities in Eastern North Carolina. *Environ. Sci. Technol.* **2025**, *59*, 2651–2664. [CrossRef] [PubMed]
3. Liu, S.; Xu, H.; Wang, J.; Ding, J.; Liu, P.; Yang, Y.; Liu, L. Evidence for global increases in urban ammonia pollution and their drivers. *Sci. Total Environ.* **2024**, *955*, 176846. [CrossRef] [PubMed]
4. Wyer, K.E.; Kelleghan, D.B.; Blanes-Vidal, V.; Schauberger, G.; Curran, T.P. Ammonia emissions from agriculture and their contribution to fine particulate matter: A review of implications for human health. *J. Environ. Manag.* **2022**, *323*, 116285. [CrossRef]
5. Zou, X.; Wang, S.; Liu, J.; Zhu, J.; Zhang, S.; Xue, R.; Gu, C.; Zhou, B. Role of gas-particle conversion of ammonia in haze pollution under ammonia-rich environment in Northern China and prospects of effective emission reduction. *Sci. Total Environ.* **2024**, *15*, 173277. [CrossRef]
6. Xenofontos, C.; Kohl, M.; Ruhl, S.; Almeida, J.; Beckmann, H.M.; Caudillo-Plath, L.; Ehrhart, S.; Höhler, K.; Sebastian, M.K.; Kong, W.; et al. The impact of ammonia on particle formation in the Asian Tropopause Aerosol Layer. *npj Clim. Atmos. Sci.* **2024**, *7*, 215. [CrossRef]
7. Behera, S.N.; Sharma, M.; Aneja, V.P.; Balasubramanian, R. Ammonia in the atmosphere: A review on emission sources, atmospheric chemistry and deposition on terrestrial bodies. *Environ. Sci. Pollut. Res.* **2013**, *20*, 8092–8131. [CrossRef]
8. Hagino, H.; Uchida, R. Effects of ammonia mitigation on secondary organic aerosol and ammonium nitrate particle formation in photochemical reacted gasoline vehicle exhausts. *Atmosphere* **2024**, *15*, 1061. [CrossRef]

9. Asman, W.A.; Sutton, M.A.; Schjørring, J.K. Ammonia: Emission, atmospheric transport and deposition. *New Phytol.* **1998**, *139*, 27–48. [CrossRef]
10. Seinfeld, J.H.; Pandis, S.P. *Atmospheric Chemistry and Physics: From Air Pollution to Climate Change*, 2nd ed.; John Wiley & Sons, Inc.: Hoboken, NJ, USA, 2006.
11. Stelson, A.W.; Seinfeld, J.H. Thermodynamic prediction of the water activity, NH_4HO_3 dissociation constant, density and refractive index for the NH_4NO_3–$(NH_4)_2SO_4H_2O$ system at 25 °C. *Atmos. Environ.* **1982**, *16*, 2507–2514. [CrossRef]
12. Stelson, A.W.; Seinfeld, J.H. Relative humidity and temperature dependence of the ammonium nitrate dissociation constant. *Atmos. Environ.* **1982**, *16*, 983–992. [CrossRef]
13. Stelson, A.W.; Seinfeld, J.H. Relative humidity and pH dependence of the vapor pressure of ammonium nitrate–nitric acid solutions at 25 °C. *Atmos. Environ.* **1982**, *16*, 993–1000. [CrossRef]
14. Theobald, M.R.; Løfstrøm, P.; Walker, J.; Andersen, H.V.; Pedersen, P.; Vallejo, A.; Sutton, M.A. An intercomparison of models used to simulate the short-range atmospheric dispersion of agricultural ammonia emissions. *Environ. Model. Softw.* **2012**, *37*, 90–102. [CrossRef]
15. Cape, J.N.; van der Eerden, L.J.; Sheppard, L.J.; Leith, I.D.; Sutton, M.A. Evidence for changing the critical level for ammonia. *Environ. Pollut.* **2009**, *157*, 1033–1037. [CrossRef] [PubMed]
16. Chen, Z.L.; Song, W.; Hu, C.C.; Chen, G.Y.; Walters, W.W.; Michalski, G.; Liu, C.Q.; Fowler, D.; Liu, X.Y. Significant contributions of combustion-related sources to ammonia emissions. *Nat. Commun.* **2022**, *13*, 7710. [CrossRef]
17. Bradow, R.L.; Stump, F.D. *Unregulated Emissions from Three-Way Catalyst Cars*; SAE Technical Paper: Pittsburgh, PA, USA, 1977; p. 770369. [CrossRef]
18. Cadle, S.H.; Nebel, G.J.; Williams, R.L. *Measurements of Unregulated Emissions from General Motors' Light-Duty Vehicles*; SAE Technical Paper: Pittsburgh, PA, USA, 1979; p. 790694. [CrossRef]
19. Urban, C.M.; Garbe, R.J. *Regulated and Unregulated Exhaust Emissions from Malfunctioning Automobiles*; SAE Technical Paper: Pittsburgh, PA, USA, 1979; p. 790696. [CrossRef]
20. Cadle, S.H.; Mulawa, P.A. Low-molecular-weight aliphatic amines in exhaust from catalyst-equipped cars. *Environ. Sci. Technol.* **1980**, *14*, 718–723. [CrossRef]
21. Smith, L.R.; Carey, P.M. *Characterization of Exhaust Emissions from High Mileage Catalyst-Equipped Automobiles*; SAE Technical Paper: Pittsburgh, PA, USA, 1982; p. 820783. [CrossRef]
22. Chang, Y.; Zou, Z.; Deng, C.; Huang, K.; Collett, J.L.; Lin, J.; Zhuang, G. The importance of vehicle emissions as a source of atmospheric ammonia in the megacity of Shanghai. *Atmos. Chem. Phys.* **2016**, *16*, 3577–3594. [CrossRef]
23. Heck, R.M.; Farrauto, R.J.; Gulati, S.T. *Catalytic Air Pollution Control: Commercial Technology*, 3rd ed.; John Wiley & Sons, Inc.: Hoboken, NJ, USA, 2009; ISBN 978-0-470-27503-0.
24. de Nevers, N. *Air Pollution Control Engineering*, 2nd ed.; Waveland Press, Inc.: Long Grove, IL, USA, 2010.
25. Johnson, T. Vehicular emissions in review. *SAE Int. J. Engines* **2016**, *9*, 1258–1275. [CrossRef]
26. Johnson, T.; Joshi, A. Review of vehicle engine efficiency and emissions. *SAE Int. J. Engines* **2018**, *11*, 1307–1330. [CrossRef]
27. Farrauto, R.J.; Deeba, M.; Alerasool, S. Gasoline automobile catalysis and its historical journey to cleaner air. *Nat. Catal.* **2019**, *2*, 603–613. [CrossRef]
28. Wang, J.; Chen, H.; Hu, Z.; Yao, M.; Li, Y. A review on the Pd-based three-way catalyst. *Catal. Rev.* **2015**, *57*, 79–144. [CrossRef]
29. Huai, T.; Durbin, T.D.; Miller, J.W.; Pisano, J.T.; Sauer, C.G.; Rhee, S.H.; Norbeck, J.M. Investigation of NH_3 emissions from new technology vehicles as a function of vehicle operating conditions. *Environ. Sci. Technol.* **2003**, *37*, 4841–4847. [CrossRef] [PubMed]
30. Heeb, N.V.; Forss, A.-M.; Brühlmann, S.; Lüscher, R.; Saxer, C.J.; Hug, P. Three-way catalyst-induced formation of ammonia—Velocity- and acceleration-dependent emission factors. *Atmos. Environ.* **2006**, *40*, 5986–5997. [CrossRef]
31. Heeb, N.V.; Saxer, C.J.; Forss, A.-M.; Brühlman, S. Trends of NO-, NO_2-, and NH_3-emissions from gasoline-fueled euro-3- to euro-4-passenger cars. *Atmos. Environ.* **2008**, *42*, 2543–2554. [CrossRef]
32. Fraser, M.P.; Cass, G.R. Detection of excess ammonia emissions from in-use vehicles and the implications for fine particle control. *Environ. Sci. Technol.* **1998**, *32*, 1053–1057. [CrossRef]
33. Czerwinski, J.; Comte, P.; Güdel, M.; Lemaire, J.; Mayer, A.; Heeb, N.; Berger, H.; Reutimann, F. Investigations of emissions of reactive substances NO_2 and NH_3 from passenger cars. *Combust. Engines* **2016**, *166*, 24–33. [CrossRef]
34. Wang, C.; Tan, J.; Harle, G.; Gong, H.; Xia, W.; Zheng, T.; Yang, D.; Ge, Y.; Zhao, Y. Ammonia formation over Pd/Rh three-way catalysts during lean-to-rich fluctuations: The effect of the catalyst aging, exhaust temperature, lambda, and duration in rich conditions. *Environ. Sci. Technol.* **2019**, *53*, 12621–12628. [CrossRef]
35. Durbin, T.D.; Pisano, J.T.; Younglove, T.; Sauer, C.G.; Rhee, S.H.; Huai, T.; Miller, J.W.; MacKay, G.I.; Hochhauser, A.M.; Ingham, M.C.; et al. The effect of fuel sulfur on NH_3 and other emissions from 2000–2001 model year vehicles. *Atmos. Environ.* **2004**, *38*, 2699–2708. [CrossRef]
36. Huang, C.; Hu, Q.; Lou, S.; Tian, J.; Wang, R.; Xu, C.; An, J.; Ren, H.; Ma, D.; Quan, Y.; et al. Ammonia Emission Measurements for Light-Duty Gasoline Vehicles in China and Implications for Emission Modeling. *Environ. Sci. Technol.* **2018**, *52*, 11223–11231. [CrossRef]

37. Sabatini, S.; Kil, I.; Hamilton, T.; Wuttke, J.; Rio, L.D.; Smith, M.; Filipi, z.; Hoffman, M.A.; Onori, S. *Characterization of Aging Effect on Three-Way Catalyst Oxygen Storage Dynamics*; SAE Technical Paper: Pittsburgh, PA, USA, 2016. [CrossRef]
38. Jeong, J.W.; Baek, S.; Park, S.; Lee, S.; Lim, Y.; Lee, K. Trends in NOx and NH_3 emissions caused by three-way catalysts. *Fuel* **2024**, *366*, 131282. [CrossRef]
39. Gao, F.; Tang, X.; Yi, H.; Zhao, S.; Li, C.; Li, J.; Shi, Y.; Meng, X. A review on selective catalytic reduction of NOx by NH_3 over Mn–based catalysts at low temperatures: Catalysts, mechanisms, kinetics and DFT calculations. *Catalysts* **2017**, *7*, 199. [CrossRef]
40. Wardana, M.K.A.; Lim, O. Review of improving the NO_X conversion efficiency in various diesel engines fitted with SCR system technology. *Catalysts* **2023**, *13*, 67. [CrossRef]
41. Twigg, M.M.; Berkhout, A.J.C.; Cowan, N.; Crunaire, S.; Dammers, E.; Ebert, V.; Gaudion, V.; Haaima, M.; Häni, C.; John, L.; et al. Intercomparison of in situ measurements of ambient NH_3: Instrument performance and application under field conditions. *Atmos. Meas. Tech.* **2022**, *15*, 6755–6787. [CrossRef]
42. Martin, N.A.; Ferracci, V.; Cassidy, N.; Hook, J.; Battersby, R.M.; di Meane, E.A.; Tang, Y.S.; Stephens, A.C.M.; Leeson, S.R.; Jones, M.R.; et al. Validation of ammonia diffusive and pumped samplers in a controlled atmosphere test facility using traceable Primary Standard Gas Mixtures. *Atmos. Environ.* **2019**, *199*, 453–462. [CrossRef]
43. Rabaud, N.E.; James, T.A.; Ashbaugh, L.L.; Flocchini, R.G. A passive sampler for the determination of airborne ammonia concentrations near large-scale animal facilities. *Environ. Sci. Technol.* **2001**, *35*, 1190–1196. [CrossRef]
44. Tang, Y.S.; Cape, J.N.; Sutton, M.A. Development and types of passive samplers for monitoring atmospheric NO_2 and NH_3 concentrations. *Sci. World J.* **2001**, *1*, 513–529. [CrossRef] [PubMed]
45. Tate, P. Ammonia Sampling Using Ogawa® Passive Samplers. Master's Thesis, University of South Florida, Tampa, FL, USA, 2002. Available online: https://digitalcommons.usf.edu/cgi/viewcontent.cgi?article=2529&context=etd (accessed on 29 March 2025).
46. Roadman, M.J.; Scudlark, J.R.; Meisinger, J.J.; Ullman, W.J. Validation of Ogawa passive samplers for the determination of gaseous ammonia concentrations in agricultural settings. *Atmos. Environ.* **2003**, *37*, 2317–2325. [CrossRef]
47. Thöni, L.; Seitler, V.; Blatter, A.; Neftel, A. A passive sampling method to determine ammonia in ambient air. *J. Environ. Monit.* **2003**, *5*, 96–99. [CrossRef]
48. Puchalski, M.A.; Sather, M.E.; Walker, J.T.; Lehmann, C.M.; Gay, D.A.; Mathew, J.; Robarge, W.P. Passive ammonia monitoring in the United States: Comparing three different sampling devices. *J. Environ. Monit.* **2011**, *13*, 3156–3167. [CrossRef]
49. Sabrina, J.; Nurulhuda, K.; Amin, A.M.; Sulaiman, M.F.; Man, H.C. Exploring use of a commercial passive sampler in a closed static chamber to measure ammonia volatilization. *Environ. Pollut.* **2022**, *315*, 120282. [CrossRef]
50. *CEN: EN 17346*; Ambient Air—Standard Method for the Determination of the Concentration of Ammonia Using Diffusive Samplers. European Committee for Standardization: Brussels, Belgium, 2020. Available online: https://www.en-standard.eu/din-en-17346-ambient-air-standard-method-for-the-determination-of-the-concentration-of-ammonia-using-diffusive-samplers/ (accessed on 25 March 2025).
51. Carmichael, G.R.; Ferm, M.; Thongboonchoo, N.; Woo, J.; Chan, L.Y.; Murano, K.; Viet, P.H.; Mossberg, C.; Bala, R.; Boonjawat, J.; et al. Measurements of sulfur dioxide, ozone and ammonia concentrations in Asia, Africa, and South America using passive samplers. *Atmos. Environ.* **2003**, *37*, 1293–1308. [CrossRef]
52. Pan, Y.; Tian, S.; Zhao, Y.; Zhang, L.; Zhu, X.; Gao, J.; Huang, W.; Zhou, Y.; Song, Y.; Zhang, Q.; et al. Identifying Ammonia Hotspots in China Using a National Observation Network. *Environ. Sci. Technol.* **2018**, *52*, 3926–3934. [CrossRef] [PubMed]
53. Yu, G.H.; Shin, H.J.; Jung, H.J.; Song, M.; Oh, S.H.; Choe, S.; Kang, G.U.; Jeon, H.; Bae, M.S. Insights into national distribution of NH_3 concentrations in Republic of Korea: Findings from passive sampler observations and implications for sources and management. *Environ. Monit. Assess.* **2024**, *196*, 121. [CrossRef]
54. Matsumoto, J.; Fujibe, F.; Takahashi, H. Urban climate in the Tokyo metropolitan area in Japan. *J. Environ. Sci.* **2017**, *59*, 54–62. [CrossRef]
55. The Ministry of Land, Infrastructure and Transport. Statistics of Japan. Survey on Motor Vehicle Fuel Consumption, Statistics code: 00600370. Available online: https://www.mlit.go.jp/k-toukei/nenryousyouhiryou.html (accessed on 25 March 2025). (In Japanese)
56. Osada, K.; Saito, S.; Tsurumaru, H.; Itahashi, S. NH_3 emissions from the human body in central Tokyo decreased during the COVID-19 pandemic lockdown. *Atmos. Environ.* **2024**, *318*, 120244. [CrossRef]
57. The Ministry of Land, Infrastructure and Transport. Road Traffic Census Vehicle Origin and Destination Survey. Available online: https://www.mlit.go.jp/road/census/r3/index.html (accessed on 25 March 2025). (In Japanese)
58. Kawasaki, S. The challenges of transportation/traffic statistics in Japan and directions for the future. *IATSS Res.* **2015**, *39*, 1–8. [CrossRef]
59. Iwafune, Y.; Ogimoto, K.; Azuma, H. Integration of electric vehicles into the electric power system based on results of road traffic census. *Energies* **2019**, *12*, 1849. [CrossRef]
60. Shibata, Y.; Morikawa, T. Review of the JCAP/JATOP air quality model study in Japan. *Atmosphere* **2021**, *12*, 943. [CrossRef]

61. Minoura, H.; Takahashi, K.; Chow, J.D.; Watson, J.G. Multi-year trend in fine and coarse particle mass, carbon, and ions in downtown Tokyo, Japan. *Atmos. Environ.* **2006**, *40*, 2478–2487. [CrossRef]
62. Takahashi, K.; Minoura, H.; Sakamoto, K. Chemical composition of atmospheric aerosols in the general environment and around a trunk road in the Tokyo metropolitan area. *Atmos. Environ.* **2008**, *42*, 113–125. [CrossRef]
63. AEROS (Ministry of the Environment). Atmospheric Environmental Regional Observation System. Available online: https://soramame.env.go.jp/ (accessed on 25 March 2025). (In Japanese)
64. Ito, A.; Wakamatsu, S.; Morikawa, T.; Kobayashi, S. 30 Years of Air Quality Trends in Japan. *Atmosphere* **2021**, *12*, 1072. [CrossRef]
65. Ogawa® Passive Samplers. Available online: http://ogawajapan.com/measurment.html (accessed on 25 March 2025). (In Japanese)
66. Japan Meteorological Agency. Japan Meteorological Agency Regional Climate Projection Data for Japan. Available online: https://search.diasjp.net/en/dataset/JMA_GWP9 (accessed on 25 March 2025). (In Japanese)
67. Ministry of the Environment. Results of Mass Concentration and Component Analysis (Manual Analysis) of Fine Particulate Matter (PM2.5). Available online: https://www.env.go.jp/air/osen/pm/monitoring.html (accessed on 25 March 2025). (In Japanese)
68. Lee, M.A.; Davies, L.; Power, S.A. Effects of roads on adjacent plant community composition and ecosystem function: An example from three calcareous ecosystems. *Environ. Pol.* **2012**, *63*, 273–280. [CrossRef]
69. Gadsdon, S.R.; Power, S.A. Quantifying local traffic contributions to NO_2 and NH_3 concentrations in natural habitats. *Environ. Pollut.* **2009**, *157*, 2845–42852. [CrossRef] [PubMed]
70. Matsumoto, R.; Yonemochi, S.; Umezawa, N.; Sakamoto, K. The influence of vehicles emission on air concentration of ammonia and nitrogen oxides at roadside. *Chikyu Kankyo* **2010**, *15*, 103–110. (In Japanese) [CrossRef]
71. Harrison, R.M.; Yin, J.; Tilling, R.M.; Cai, X.; Seakins, P.W.; Hopkins, J.R.; Lansley, D.L.; Lewis, A.C.; Hunter, M.C.; Heard, D.E.; et al. Measurement and modelling of air pollution and atmospheric chemistry in the U.K. west midlands conurbation: Overview of the PUMA consortium project. *Sci. Total Environ.* **2006**, *360*, 5–25. [CrossRef]
72. Perrino, C.; Catrambone, M.; Di Menno di Bucchianico, A.; Allegrini, I. Gaseous ammonia in the urban area of Rome, Italy and its relationship with traffic emissions. *Atmos. Environ.* **2002**, *36*, 5385–5394. [CrossRef]
73. Wentworth, G.R.; Murphy, J.G.; Gregoire, P.K.; Cheyne, C.A.L.; Tevlin, A.G.; Hems, R. Soil–atmosphere exchange of ammonia in a non-fertilized grassland: Measured emission potentials and inferred fluxes. *Biogeosciences* **2014**, *11*, 5675–5686. [CrossRef]
74. Osada, K. Measurement report: Short-term variation in ammonia concentrations in an urban area increased by mist evaporation and emissions from a forest canopy with bird droppings. *Atmos. Chem. Phys.* **2020**, *20*, 11941–11954. [CrossRef]
75. Minoura, H.; Ito, A. Observation of the primary NO_2 and NO oxidation near the trunk road in Tokyo. *Atmos. Environ.* **2010**, *44*, 23–29. [CrossRef]
76. Takekawa, H.; Chatani, S.; Ito, A. A new approach for estimation of the effect of NOx emission reduction on roadside NO_2 concentration in Tokyo. *Atmos. Environ.* **2013**, *68*, 92–102. [CrossRef]
77. Battye, W.; Aneja, V.P.; Roelle, P.A. Evaluation and improvement of ammonia emissions inventories. *Atmos. Environ.* **2003**, *37*, 3873–3883. [CrossRef]
78. Aguilar-Dodier, L.C.; Castillo, J.E.; Quintana, P.J.; Montoya, L.D.; Molina, L.T.; Zavala, M.; Almanza-Veloz, V.; Rodríguez-Ventura, J.G. Spatial and temporal evaluation of H_2S, SO_2 and NH_3 concentrations near Cerro Prieto geothermal power plant in Mexico. *Atmos. Pollut. Res.* **2020**, *11*, 94–104. [CrossRef]
79. Gu, M.; Pan, Y.; Walters, W.W.; Sun, Q.; Song, L.; Wang, Y.; Xue, Y.; Fang, Y. Vehicular emissions enhanced ammonia concentrations in winter mornings: Insights from diurnal nitrogen isotopic signatures. *Environ. Sci. Technol.* **2022**, *56*, 1578–1585. [CrossRef]
80. Farren, N.J.; Davison, J.; Rose, R.A.; Wagner, R.L.; Carslaw, D.C. Underestimated ammonia emissions from road vehicles. *Environ. Sci. Technol.* **2020**, *54*, 15689–15697. [CrossRef] [PubMed]
81. Reche, C.; Viana, M.; Pandolfi, M.; Alastuey, A.; Moreno, T.; Amato, F.; Ripoll, A.; Querol, X. Urban NH_3 levels and sources in a Mediterranean environment. *Atmos. Environ.* **2012**, *57*, 153–164. [CrossRef]
82. Yamamoto, T.; Sekine, Y.; Sohara, K.; Nakai, S.; Yanagisawa, Y. Effect of heating temperature on ammonia emission in the mainstream aerosols from heated tobacco products. *Toxics* **2022**, *10*, 592. [CrossRef] [PubMed]
83. Zhou, Y.; Zheng, N.; Luo, L.; Zhao, J.; Qu, L.; Guan, H.; Xiao, H.; Zhang, Z.; Tian, J.; Xiao, H. Biomass burning related ammonia emissions promoted a self-amplifying loop in the urban environment in Kunming (SW China). *Atmos. Environ.* **2020**, *253*, 118138. [CrossRef]
84. Alnajideen, M.; Shi, H.; Northrop, W.; Emberson, D.; Kane, S.; Czyzewski, P.; Alnaeli, M.; Mashruk, S.; Rouwenhorst, K.; Yu, C.; et al. Ammonia combustion and emissions in practical applications: A review. *Carbon Neutrality* **2024**, *3*, 13. [CrossRef]
85. Nadimi, E.; Przybyła, G.; Lewandowski, M.T.; Adamczyk, W. Effects of ammonia on combustion, emissions, and performance of the ammonia/diesel dual-fuel compression ignition engine. *J. Energy Inst.* **2023**, *107*, 101158. [CrossRef]

86. Air Quality Consultants. Ammonia Emissions from Roads for Assessing Impacts on Nitrogen-Sensitive Habitats. February 2020. Available online: https://infrastructure.planninginspectorate.gov.uk/wp-content/ipc/uploads/projects/TR010030/TR010030-000742-Royal%20Horticulture%20Society%20-%20Appendix%20D%20Ammonia-from-Roads-for-Habitats-Assessments.pdf (accessed on 25 March 2025).
87. Singh, R.; Kim, K.; Park, G.; Kang, S.; Park, T.; Ban, J.; Choi, S.; Song, J.; Yu, D.-G.; Woo, J.-H.; et al. Seasonal and Spatial Variations of Atmospheric Ammonia in the Urban and Suburban Environments of Seoul, Korea. *Atmosphere* **2021**, *12*, 1607. [CrossRef]
88. Chang, Y.; Liu, X.; Deng, C.; Dore, A.J.; Zhuang, G. Source apportionment of atmospheric ammonia before, during, and after the 2014 APEC summit in Beijing using stable nitrogen isotope signatures. *Atmos. Chem. Phys.* **2016**, *16*, 11635–11647. [CrossRef]
89. Yao, X.; Zhang, L. Trends in atmospheric ammonia at urban, rural, and remote sites across North America, Atmos. *Chem. Phys.* **2016**, *16*, 11465–11475. [CrossRef]
90. Cao, J.J.; Zhang, T.; Chow, J.C.; Watson, J.G.; Wu, F.; Li, H. Characterization of atmospheric ammonia over Xi'an, China. *Aerosol Air Qual. Res.* **2009**, *9*, 277–289. [CrossRef]
91. Meng, Z.Y.; Lin, W.L.; Jiang, X.M.; Yan, P.; Wang, Y.; Zhang, Y.M.; Jia, X.F.; Yu, X.L. Characteristics of atmospheric ammonia over Beijing, China. *Atmos. Chem. Phys.* **2011**, *11*, 6139–6151. [CrossRef]
92. Zhou, C.; Zhou, H.; Holsen, T.M.; Hopke, P.K.; Edgerton, E.S.; Schwab, J.J. Ambient ammonia concentrations across New York State. *J. Geophys. Res. Atmos.* **2019**, *124*, 8287–8302. [CrossRef]
93. Li, Y.; Thompson, T.M.; Van Damme, M.; Chen, X.; Benedict, K.B.; Shao, Y.; Day, D.; Boris, A.; Sullivan, A.P.; Ham, J.; et al. Temporal and spatial variability of ammonia in urban and agricultural regions of northern Colorado, United States. *Atmos. Chem. Phys.* **2017**, *17*, 6197–6213. [CrossRef]
94. Oh, S.; Kim, S.-G.; Lee, J.B.; Park, J.; Jee, J.-B.; Hong, S.-W.; Kwon, K.-S.; Song, M. Spatial distributions of atmospheric ammonia in a rural area in South Korea and the associated impact on a nearby urban area. *Atmosphere* **2021**, *12*, 1411. [CrossRef]
95. Wilson, S.M.S.; Serre, M.L. Use of passive samplers to measure ammonia levels in a high-density industrial hog farm area of North Carolina. *Atmos. Environ.* **2007**, *41*, 607–6086. [CrossRef]
96. López-Aizpún, M.; Arango-Mora, C.; Santamaría, C.; Lasheras, E.; Santamaría, J.; Ciganda, V.; Cárdenas, L.; Elustondo, D. Atmospheric ammonia concentration modulates soil enzyme and microbial activity in an oak forest affecting soil microbial biomass. *Soil Biol. Biochem.* **2018**, *116*, 378–387. [CrossRef]
97. Osada, K.; Saito, S.; Tsurumaru, H.; Hoshi, J. Vehicular exhaust contributions to high NH_3 and $PM_{2.5}$ concentrations during winter in Tokyo, Japan. *Atmos. Environ.* **2019**, *206*, 218–224. [CrossRef]
98. Kean, A.J.; Harley, R.A.; Littlejohn, D.; Kendall, G.R. On-road measurement of ammonia and other motor vehicle exhaust emissions. *Environ. Sci. Technol.* **2000**, *34*, 3535–3539. [CrossRef]
99. Emmenegger, L.; Mohn, J.; Sigrist, M.; Marinov, D.; Steinemann, U.; Zumsteg, F.; Meier, M. Measurement of ammonia emissions using various techniques in a comparative tunnel study. *Int. J. Environ. Pollut.* **2004**, *22*, 326–341. [CrossRef]
100. Vieira-Filho, M.S.; Ito, D.T.; Pedrotti, J.J.; Coelho, L.H.G.; Fornaro, A. Gas-phase ammonia and water-soluble ions in particulate matter analysis in an urban vehicular tunnel. *Environ. Sci. Pollut. Res.* **2016**, *23*, 19876–19886. [CrossRef] [PubMed]
101. Liu, T.; Wang, X.; Wang, B.; Ding, X.; Deng, W.; Lü, S.; Zhang, Y. Emission factor of ammonia (NH_3) from on-road vehicles in China: Tunnel tests in urban Guangzhou. *Environ. Res. Lett.* **2014**, *9*, 064027. [CrossRef]
102. Baum, M.M.; Kiyomiya, E.S.; Kumar, S.; Lappas, A.M.; Kapinus, V.A.; Lord, H.C., III. Multicomponent remote sensing of vehicle exhaust by dispersive absorption spectroscopy. 2. Direct on road ammonia measurements. *Environ. Sci. Technol.* **2001**, *35*, 3735–3741. [CrossRef]
103. Durbin, T.D.; Wilson, R.D.; Norbeck, J.M.; Miller, J.W.; Huai, T.; Rhee, S.H. Estimates of the emission rates of ammonia from light-duty vehicles using standard chassis dynamometer test cycles. *Atmos. Environ.* **2002**, *36*, 1475–1482. [CrossRef]
104. Karlsson, H.L. Ammonia, nitrous oxide and hydrogen cyanide emissions from five passenger vehicles. *Sci. Total Environ.* **2004**, *334–335*, 125–132. [CrossRef]
105. Livingston, C.; Rieger, P.; Winer, A. Ammonia emissions from a representative in-use fleet of light and medium-duty vehicles in the California South Coast Air Basin. *Atmos. Environ.* **2009**, *43*, 3326–3333. [CrossRef]
106. Suarez-Bertoa, R.; Zardini, A.A.; Astorga, C. Ammonia exhaust emissions from spark ignition vehicles over the New European Driving Cycle. *Atmos. Environ.* **2014**, *97*, 43–53. [CrossRef]
107. Suarez-Bertoa, R.; Mendoza-Villafuerte, P.; Riccobono, F.; Vojtisek, M.; Pechout, M.; Perujo, A.; Astorga, C. On-road measurement of NH3 emissions from gasoline and diesel passenger cars during real world driving conditions. *Atmos. Environ.* **2017**, *166*, 488–497. [CrossRef]
108. Selleri, T.; Melas, A.; Bonnel, P.; Suarez-Bertoa, R. NH_3 and CO emissions from fifteen Euro 6d and Euro 6d-TEMP gasoline-fuelled vehicles. *Catalysts* **2022**, *12*, 245. [CrossRef]
109. Suarez-Bertoa, R.; Pechout, M.; Vojtíšek, M.; Astorga, C. Regulated and non-regulated emissions from Euro 6 diesel, gasoline and CNG vehicles under real-world driving conditions. *Atmosphere* **2020**, *11*, 204. [CrossRef]

110. Chatani, S.; Kitayama, K.; Itahashi, S.; Irie, H.; Shimadera, H. Effectiveness of emission controls implemented since 2000 on ambient ozone concentrations in multiple timescales in Japan: An emission inventory development and simulation study. *Sci. Total Environ.* **2023**, *894*, 165058. [CrossRef] [PubMed]
111. Davison, J.; Bernard, Y.; Borken-Kleefeld, J.; Farren, N.J.; Hausberger, S.; Sjödin, Å.; Tate, J.E.; Vaughan, A.R.; Carslaw, D.C. Distance-based emission factors from vehicle emission remote sensing measurements. *Sci. Total Environ.* **2020**, *739*, 139688. [CrossRef]
112. Pant, P.; Harrison, R.M. Estimation of the contribution of road traffic emissions to particulate matter concentrations from field measurements: A review. *Atmos. Environ.* **2013**, *77*, 78–97. [CrossRef]
113. Ministry of Environment, Japan. Guidelines for Calculating Total Greenhouse Gas Emissions. 2007. Available online: https://www.env.go.jp/policy/local_keikaku/data/guideline.pdf (accessed on 25 March 2025). (In Japanese)
114. Ministry of Land, Infrastructure, Transport and Tourism. Automobile Fuel Consumption Survey. 2017. Available online: https://www.e-stat.go.jp/stat-search/files?page=1&layout=datalist&cycle=8&toukei=00600370&tstat=000001051698&tclass1val=0&year=20171&month=0&result_back=1 (accessed on 25 March 2025). (In Japanese)
115. Ministry of Environment, Japan. Other-Urea Used as a Catalyst. Detailed Information on the Calculation Method for Greenhouse Gas Emissions and Sinks. 2024. Available online: https://www.env.go.jp/content/000273300.pdf (accessed on 25 March 2025). (In Japanese)
116. Automobile Inspection and Registration Information Association. Automobile Ownership Trends in Japan. Available online: https://www.airia.or.jp/publish/statistics/trend.html (accessed on 25 March 2025). (In Japanese)
117. Teng, X.; Hu, Q.; Zhang, L.; Qi, J.; Shi, J.; Xie, H.; Gao, H.; Yao, X. Identification of major sources of atmospheric NH_3 in an urban environment in Northern China during wintertime. *Environ. Sci. Technol.* **2017**, *51*, 6839–6848. [CrossRef]
118. Japan Automobile Manufacturers Association, Inc. The Motor Industry of Japan. 2024. Available online: https://www.jama.or.jp/english/reports/docs/MIoJ2024_e.pdf (accessed on 25 March 2025).
119. European Union Law. Proposal for a Directive of the European Parliament and of the Council on Ambient Air Quality and Cleaner Air for Europe (Recast). Document 52022PC0542. Official Journal of the European Union. 2022. Available online: https://eur-lex.europa.eu/legal-content/EN/TXT/?uri=COM:2022:0542:FIN (accessed on 25 March 2025).